THE AMERICAN MINERALOGIST, VOL. 50, JULY-AUGUST, 1965

CHLORITE POLYTYPISM: III. CRYSTAL STRUCTURE OF AN ORTHOHEXAGONAL IRON CHLORITE

HARUO SHIROZU[1] AND S. W. BAILEY, *Department of Geology, University of Wisconsin, Madison, Wisconsin.*

ABSTRACT

Iron chlorite from the Tazawa mine, Japan, $2[(Mg_{1.3}Fe_{3.4}^{2+}Al_{1.3})(Si_{2.7}Al_{1.3})O_{10}(OH)_8]$, is an orthohexagonal I*b* semirandom stacking type with $a=5.390$ Å, $b=9.336$ Å, $c=14.166$ Å, $\beta=90°$. The structure of a single chlorite layer ($C2/m$), in which the brucite sheet is rotated by 180° relative to its orientation in the more common II*b* type layer, has been refined. The results indicate that the talc network is distorted by 5° tetrahedral rotations in a direction to form a favorable hydrogen bond system between the talc and brucite sheets. This direction is in the opposite sense, relative to the talc octahedral cations, to that found in most layer silicates. Sixty per cent of the octahedral iron is concentrated in the talc sheet. The temperature parameters of the octahedral cations are strikingly anisotropic, the thermal vibrations being larger parallel to the Z axis. The intensity distribution along the $k\neq 3n$ streaks parallel to the Z* direction indicates the existence of random layer rotations of 120° in addition to random $b/3$ layer displacements parallel to the three pseudohexagonal Y axes.

The relative abundances of the chlorite polytypes described in Part I are reconsidered in the light of the present results, and explained by the relative amounts of repulsion and attraction between the ions in the structures.

INTRODUCTION

Part I of this study of chlorite polytypism (Bailey and Brown, 1962) showed that four chlorite layer types with different ways of superposition of the talc and brucite sheets are theoretically possible and that layers of the same type may be superimposed to form twelve regular one-layer polytypes and six semirandom structures. Semirandom stacking is defined as an irregular sequence along Z* of the three relative stacking positions that permit hydrogen bonding between the brucite and talc surfaces and that are related by shifts of $\pm b/3$ along the three pseudohexagonal Y axes. For each semirandom structure there are three regular one-layer polytypes, two of which are always equivalent or enantiomorphic. The powder pattern of a regular polytype is usually not distinguishable from that of its related semirandom structure because of the weakness of the diagnostic $k\neq 3n$ reflections. For this reason it is convenient to classify the regular polytypes, including most of the regular two- and three-layer forms known so far, according to the geometry of the semirandom structures. In the terminology of Bailey and Brown these are the I*a*, I*b*, II*a*, and II*b* structures with monoclinic-shaped cells and the I*b* and II*a* structures with orthorhombic-shaped cells. The semirandom structures occur in more abundance than the regular polytypes.

[1] Present address: Department of Geology, Kyushu University, Fukuoka, Japan.

Of the six theoretical semirandom assemblages, only the two II*a* structures have not yet been recognized in nature.

Many structural studies of the common II*b* layer type have been made and the structure of a regular I*a* polytype was described as Part II of this study (Brown and Bailey, 1963). A chlorite believed to be the orthohexagonal I*b* type in question in this paper was studied by von Engelhardt (1942), who found the powder pattern of a "chamosite" from Schmiedefeld could be indexed on the basis of an orthorhombic-shaped cell. He proposed a structure having an orientation relation between the talc and brucite sheets similar to that of the common II*b* chlorite, but with no shift between these sheets of $a/3$ along the X axis.

The structure of von Engelhardt does not have an optimum hydrogen bond arrangement between the brucite and talc sheets, and a more plausible structure giving better agreement between the calculated and observed $h0l$ structure amplitudes was proposed in Part I. In this proposed I*b* structure the brucite sheet is rotated by 180° relative to its orientation in the common II*b* type layer and is positioned on top of the talc sheet so that the octahedral talc and brucite cations superimpose vertically. The present refinement was made to verify the I*b* structure and to learn more about the bond lengths, interatomic forces, and layer distortions in this chlorite. Although over 100 crystals from several different localities were examined, no crystals with regular layer sequences were found. It has only been possible to determine the average structure within a I*b* chlorite layer by refinement using the sharp $k=3n$ reflections. The nature of the semirandom stacking of adjacent layers has been deduced from the intensity distribution along the $k\neq 3n$ streaks. The results confirm the postulated orthohexagonal I*b* structure and also indicate the necessity of some modification of the interpretation in Part I as to polytype relative stabilities.

Experimental Work

Throughout this investigation an iron-rich chlorite from the Tazawa mine, Akita Prefecture, Japan, was used, which gives a powder pattern very similar to those of the orthohexagonal iron chlorites described by Shirozu (1958). The chlorite occurs as lath-shaped flakes in hemispherical aggregates with *b*-axis disordered kaolinite in a hydrothermal quartz-copper vein.

Although the diffraction spots with $k=3n$ are sharp in the single crystal photographs of certain crystals, the reflections with $k\neq 3n$ of every crystal are a complete streak parallel to the Z* axis, which makes it impossible to choose the true X and Y axes of the unit cell as well as the three-dimensional space group. The diffraction patterns about the

Z* axis have trigonal symmetry, which indicates the equivalence of the [010], [310], and [$3\bar{1}0$] directions, but the overall symmetry of the structure must be monoclinic or triclinic according to the arguments in Part I. The morphologically unique direction of the three possible Y axes, namely the elongation direction of the lath-shaped crystal, was assumed as true Y, and an orthorhombic-shaped cell with monoclinic symmetry, $C2/m$, was selected to examine the structure within a single chlorite layer. No justification for any lower symmetry is given by the $k=3n$ reflections.

On oscillation and precession photographs pairs of reflections having the same *hkl* index but different *l* signs have almost identical intensities in certain crystals and simulate orthorhombic symmetry. This has been found to be due to a twinning on (001) related by 180° rotation about either the X or Z axes. The differences between the intensities of the *hkl* pairs are variable from crystal to crystal. Therefore, a thin flake (dimensions .07×.20×.008 mm) giving the greatest intensity differences within the *hkl* pairs was used in collecting the intensity data for the structure determination. Even this crystal was partially twinned, as revealed in the course of refinement.

The cell dimensions determined by the θ-method of Weisz, Cochran, and Cole (1948) are $a=5.390\pm0.002$ Å, $b=9.336\pm0.005$ Å, $c=14.166\pm0.005$ Å, $\beta=90.00\pm0.05°$, V=712.85 Å; b is exactly $a\sqrt{3}$. The unit cell formula estimated from these dimensions by use of the x-ray spacing graphs of Shirozu (1958) is $2[(Mg_{1.3}Fe_{3.4}{}^{2+}Al_{1.3})\ (Si_{2.7}Al_{1.3})O_{10}(OH)_8]$, which was used for the structure factor calculations. According to Foster's (1962) classification the chlorite is a ripidolite.

Intensity data for 247 observed reflections were collected by means of multiple film pack Weissenberg photographs of *h0l*, *h3l*, and *h6l* reciprocal levels taken with CuKα radiation. Because of the small size of the crystal, exposure times of 160 hours were required. The intensities of the sharp $k=3n$ spots and of the $k\neq3n$ streaks were estimated visually by comparison with a standard multiple scale and were corrected for the Lorentz-polarization factor. The photographs show an appreciable Wells effect because of the large linear absorption coefficient of 345/cm for copper radiation. An absorption correction was made by a graphical means based on the transmission factors calculated by Joel, Vera, and Garaycochea's method (1953). Weissenberg photographs were taken also with CoKα and MoKα radiations. These were useful to confirm the absorption corrections because the maximum absorption effects for a thin flake are given by reflections with different indices for the different radiations.

Of the *h0l* structure amplitude data calculated by Bailey and Brown (1962) for the six chlorite structures, those of the I*b* ($\beta=90°$) assemblage

agree best with the observed *h0l* structure amplitudes, although there are minor discrepancies due to the high Fe content of our specimen. The three regular one-layer polytypes possible with this assemblage are I*b*-1 ($\beta = 90°$, $C2/m$), I*b*-3 ($\alpha = 102°$, $C\bar{1}$), and I*b*-5 ($\alpha = 102°$, $C\bar{1}$), all of which have an identical atomic arrangement within a single chlorite layer, have an identical [010] projection, and give identical intensities for the reflections with $k = 3n$ (although the l indices change as the α angle changes. Atomic parameters from the I*b*-1 model were used to place the observed structure amplitudes on an absolute scale and to initiate refinement.

Refinement of a Single Chlorite Layer

Refinement of the structure was carried out using the Larson-Cromer full matrix least squares and Fourier summation programs (Los Alamos Scientific Laboratory) as modified by J. J. Finney and R. A. Eggleton for use on the Wisconsin CDC 1604 computer.

The regular stacking I*b*-1 model contains eleven crystallographically independent atoms in the unit cell. In the present structure, which has semirandom stacking, the atoms repeating at intervals of $b/3$ are statistically equivalent, *i.e.* indistinguishable by reflections with $k = 3n$. These atoms were grouped together, therefore, and their y parameters were fixed as in Table 2. In the first stage of refinement by the least squares method, eleven positional parameters and seven isotropic thermal parameters were allowed to vary, and the octahedral scattering matter was assumed to be distributed equally between the talc and brucite sheets. Only the observed reflections were used, and an arbitrary weighting system was used in which smaller weights were given to the reflections with small transmission factors and with very small or very large F values.

The initial least squares cycle and F_o-F_c [010] projection showed definite shifts of the basal oxygens of the tetrahedral network, uneven distribution of the octahedral cations between the talc and brucite sheets, and thermal anisotropy of the octahedral cations. Although further least squares refinement, in which the uneven distribution and the anisotropic thermal parameters of the octahedral cations were taken into account, gave a reliability factor of $R = 12.8\%$, there remained several reflections having unreasonable discrepancies between F_o and F_c values. Comparison at this stage of the F_o and F_c values of *hkl* index pairs involving opposite l signs showed a quantitative relationship that could best be explained by a 9% volume of the (001) twinning previously mentioned. Although the twinning affects all reflections, it is most evident in those cases where a strong twin reflection is superim-

posed on a weak reflection from the main portion of the crystal. A twinning correction was made and proved reasonable, judging from the improved agreement of the F_o and F_c values and reduced R values during subsequent refinement. The final reliability factor was R=8.7%. The final F_o and F_c values are listed in Table 1. Table 2 contains the final atomic coordinates and temperature factors. Table 3 contains bond lengths and angles computed from these coordinates.

Interpretation of Streaks with $k \neq 3n$

The [010] projection of a layer silicate is usually identical with the [310] and [3$\bar{1}$0] projections in the ideal scheme, even after taking the distortion of the hexagonal network into account. In the case of the Tazawa chlorite overall equivalences are recognized between reflections with the following indices: 20l and 13$\bar{l}$; 40l and 26$\bar{l}$; 60l and 39$\bar{l}$; 33l, 06l, and 33$\bar{l}$; 53l, 19l and 46$\bar{l}$. This means that the reflections with $k=3n$ are not affected by possible rotations of 120° about the Z* axis (coincident with the Z axis in this stucture). Any rotations that may occur have to be determined from the reflections with $k \neq 3n$.

It has been stated previously that streaking of the $k \neq 3n$ reflections parallel to the Z* axis indicates random $b/3$ layer displacements parallel to the three Y axes. The randomness may be restricted to linear displacements so that the direction of stagger of each of the talc sheets is maintained constant along one of the three X axes. In this case the intensity distributions along the $k \neq 3n$ streaks should change in accordance with the variation of the structure amplitudes along the reciprocal rods parallel to Z*. This is the observed situation for the La Capelada Cr-chlorite examined by Garrido (1949). Figure 1*c–e* illustrates for a I*b* type layer how the intensity should vary with increasing l value (nonintegral) for the 02l, 1$\bar{1}l$, and $\bar{1}\bar{1}l$ streaks (120° apart) if only linear $b/3$ interlayer displacements along the three Y axes are involved. This intensity distribution should be very similar for all layer types because only the tetrahedral cations and basal oxygens are involved. The observed intensity distribution for our specimen (Fig. 1a) agrees only with the mean (Fig. 1b) of these three calculated F^2 curves, and can be explained only by superposition of the three directions by 120° layer rotations. Layer rotations of 120° are geometrically equivalent to the three $a/3$ shifts that are possible at the octahedral junction within the talc sheets. Although these shifts are along the three X axes, the resulting positions are related to *each other* by displacements of $\pm b/3$ along the three Y axes.

The observed intensity distribution along $k \neq 3n$ streaks for the Tazawa I*b* chlorite probably can be explained solely by 120° layer rotations,

TABLE 1. OBSERVED AND CALCULATED STRUCTURE AMPLITUDES

H	K	L	Fo	Fc	H	K	L	Fo	Fc	H	K	L	Fo	Fc	H	K	L	Fo	Fc
0	0	2	167	169	4	0	12	48	52	1	3	−13	22	17	0	6	6	89	83
0	0	3	98	−93	4	0	14	36	47	1	3	−14	24	13	0	6	7	22	−24
0	0	4	240	242	4	0	−1	71	65	1	3	−15	11	−11	0	6	8	18	8
0	0	5	113	104	4	0	−2	209	197	1	3	−16	64	63	0	6	9	11	8
0	0	6	40	33	4	0	−3	16	−7	1	3	−17	25	31	0	6	10	108	108
0	0	7	64	−62	4	0	−4	92	92	3	3	0	292	254	0	6	11	40	35
0	0	8	39	38	4	0	−5	5	−4	3	3	1	39	30	0	6	12	71	59
0	0	9	51	48	4	0	−6	150	169	3	3	2	155	143	0	6	13	29	−23
0	0	10	125	127	4	0	−7	31	33	3	3	3	46	−40	0	6	14	63	62
0	0	11	27	27	4	0	−8	62	67	3	3	4	107	106	0	6	15	22	23
0	0	12	106	101	4	0	−9	30	−28	3	3	5	50	47	2	6	0	53	52
0	0	13	11	−10	4	0	−10	34	31	3	3	6	84	91	2	6	1	71	61
0	0	14	99	79	4	0	−11	11	11	3	3	7	21	−21	2	6	2	214	202
0	0	15	11	14	4	0	−12	44	46	3	3	8	16	11	2	6	3	21	−6
0	0	16	92	77	4	0	−13	16	14	3	3	10	100	114	2	6	4	90	95
0	0	18	13	2	4	0	−14	26	25	3	3	11	39	39	2	6	5	16	−10
2	0	0	75	81	6	0	0	133	120	3	3	12	65	63	2	6	6	139	171
2	0	1	41	38	6	0	1	32	26	3	3	13	26	−24	2	6	7	38	32
2	0	2	316	291	6	0	2	72	67	3	3	14	65	66	2	6	8	66	70
2	0	3	43	42	6	0	3	30	−26	3	3	15	21	25	2	6	9	31	−32
2	0	4	210	213	6	0	4	55	57	3	3	−1	38	28	2	6	10	36	33
2	0	5	49	−47	6	0	5	33	33	3	3	−2	155	143	2	6	11	14	10
2	0	6	218	230	6	0	6	62	61	3	3	−3	46	−37	2	6	12	46	50
2	0	7	61	67	6	0	7	15	−16	3	3	−4	108	108	2	6	13	18	12
2	0	8	127	131	6	0	8	12	11	3	3	−5	51	47	2	6	14	25	29
2	0	9	53	−56	6	0	−1	19	10	3	3	−6	86	87	2	6	−1	75	−68
2	0	10	16	12	6	0	−2	69	64	3	3	−7	21	−21	2	6	−2	64	62
2	0	11	21	22	6	0	−3	16	−11	3	3	−8	16	7	2	6	−3	71	71
2	0	12	78	84	6	0	−4	56	63	3	3	−10	99	109	2	6	−4	98	101
2	0	13	21	18	6	0	−5	20	21	3	3	−11	37	39	2	6	−5	29	−28
2	0	14	27	18	6	0	−6	50	51	3	3	−12	63	58	2	6	−6	46	58
2	0	15	11	−11	6	0	−7	8	−7	3	3	−13	26	−23	2	6	−7	18	19
2	0	16	62	63	6	0	−8	12	13	3	3	−14	65	63	2	6	−8	138	145
2	0	17	26	30	1	3	0	77	77	3	3	−15	18	26	2	6	−9	27	23
2	0	−1	39	−34	1	3	1	39	−34	5	3	0	61	62	2	6	−10	80	82
2	0	−2	53	43	1	3	2	51	45	5	3	1	35	30	2	6	−11	21	−18
2	0	−3	50	52	1	3	3	50	49	5	3	2	130	124	2	6	−12	52	50
2	0	−4	127	126	1	3	4	121	129	5	3	3	15	10	2	6	−13	6	5
2	0	−5	16	15	1	3	5	15	17	5	3	4	86	88	2	6	−14	38	46
2	0	−6	88	97	1	3	6	92	103	5	3	5	18	−11	4	6	0	65	59
2	0	−7	15	−9	1	3	7	16	−12	5	3	6	95	103	4	6	1	43	−32
2	0	−8	182	205	1	3	8	187	207	5	3	7	31	29	4	6	2	47	40
2	0	−9	56	61	1	3	9	53	61	5	3	8	69	74	4	6	3	36	32
2	0	−10	124	133	1	3	10	129	137	5	3	9	21	−21	4	6	4	95	93
2	0	−11	42	−47	1	3	11	44	−50	5	3	10	15	15	4	6	6	38	42
2	0	−12	57	54	1	3	12	56	53	5	3	11	8	5	4	6	7	15	−4
2	0	−13	22	21	1	3	13	21	21	5	3	−1	40	−29	4	6	8	107	112
2	0	−14	75	70	1	3	14	74	73	5	3	−2	45	38	4	6	9	34	33
2	0	−16	19	−9	1	3	16	18	−9	5	3	−3	34	32	4	6	10	56	65
2	0	−17	6	−10	1	3	17	7	−10	5	3	−4	85	89	4	6	11	25	−26
4	0	0	49	51	1	3	−1	39	35	5	3	−5	7	1	4	6	−1	38	30
4	0	1	74	−68	1	3	−2	294	288	5	3	−6	27	36	4	6	−2	131	122
4	0	2	64	60	1	3	−3	42	43	5	3	−7	4	−4	4	6	−3	20	7
4	0	3	74	74	1	3	−4	198	210	5	3	−8	100	108	4	6	−4	84	82
4	0	4	103	107	1	3	−5	45	−49	5	3	−9	34	36	4	6	−5	19	−10
4	0	5	30	−26	1	3	−6	199	230	5	3	−10	54	61	4	6	−6	91	104
4	0	6	64	62	1	3	−7	65	69	5	3	−11	21	−25	4	6	−7	36	29
4	0	7	22	20	1	3	−8	119	130	0	6	1	28	27	4	6	−8	61	69
4	0	8	132	150	1	3	−9	49	−58	0	6	2	135	136	4	6	−9	26	−21
4	0	9	30	24	1	3	−10	17	9	0	6	3	46	−42	4	6	−10	19	14
4	0	10	78	84	1	3	−11	22	23	0	6	4	108	105	4	6	−11	9	6
4	0	11	16	−18	1	3	−12	77	83	0	6	5	50	46					

TABLE 2. POSITIONAL AND TEMPERATURE PARAMETERS WITH STANDARD DEVIATIONS

Atom	Parameter		σ	Atom	Parameter		σ
$2M_1$, $4M_2$	x	.0	.0	8T	x	.3328	.0009
$[Fe_{.67}(Mg, Al)_{.33}]$	y	.0, 1/3	.0	$(Si_{.67}Al_{.33})$	y	1/3	.0
	z	.0	.0		z	.1949	.0004
	B_{11}	.0074	.0011		B	1.42	.11
	B_{22}	.0035	.0015				
				$8O_1$, $4(OH)_1$	x	.3349	.0015
	B_{33}	.0029	.0002		y	1/3,.0	.0
	B_{12}	−.0020	.0026		z	.0770	.0006
	B_{13}	−.0008	.0007		B	1.89	.19
	B_{23}	.0002	.0007				
				$8O_2$	x	.094	.003
$2M_3$, $4M_4$	x	.0	.0		y	.236	.003
$[Fe_{.47}(Mg,Al)_{.53}]$	y	.0, 1/3	.0		z	.236	.001
	z	.5	.0		B	2.13	.34
	B_{11}	.0082	.0012				
	B_{22}	.0027	.0017	$4O_3$	x	.310	.004
	B_{33}	.0029	.0002		y	1/2	.0
	B_{12}	−.0018	.0029		z	.236	.002
	B_{13}	−.0010	.0008		B	1.51	.47
	B_{23}	−.0001	.0008	$8(OH)_2$, $4(OH)_3$	x	.1656	.0017
					y	1/6, 1/2	.0
					z	.4303	.0007
					B	2.58	.21

without calling at all upon linear interlayer displacements along the Y axes. But it is considered unlikely that random 120° rotations would take place if the layer stacking were strictly regular or that regular 120° rotations would take place if random layer displacement were involved. A combination of shifts within the talc sheets (equivalent to rotations) and between talc sheets is most likely. Thus the refined structure is an average structure from several points of view and it is possible that, in addition to the *y* coordinates already mentioned, the *x* parameters of T, of O_1 and $(OH)_1$, and of $(OH)_2$ and $(OH)_3$ in Table 2 should be replaced by ideal values of $\frac{1}{3}$, $\frac{1}{3}$, and $\frac{1}{6}$ respectively. The coordinates determined by refinement for these atoms differ from the ideal values by less than one standard deviation.

It was assumed erroneously in Part I, because of the existence of unique layer types even in semirandom stacking systems, that the brucite sheet always maintains one fixed position (*a* or *b*) on top of the talc sheet below. Garrido (1949) makes a similar assumption for the Cr-chlorite he examined. Further analysis of random interlayer shift systems, however, shows that this relationship is not necessary to explain the

TABLE 3. INTERATOMIC DISTANCES WITH MAXIMUM DIRECTIONAL STANDARD DEVIATIONS IN Å AND BOND ANGLES IN DEGREES

Bond length	σ_m		Bond length	σ_m
$T-O_1$	1.670	.006	O_1-O_2	2.732, 2.760 .020
$T-O_2$	1.656, 1.684	.020	O_1-O_3	2.744 .018
$T-O_3$	1.668	.017	O_2-O_2	2.708 .027
Mean	1.670		O_2-O_3	2.681, 2.728 .026
			Mean	2.726
M_1, M_2-O_1	2.098×4, 2.109×2	.006		
$M_1, M_2-(OH)_1$				
Mean	2.102			
$M_3, M_4-(OH)_2$	2.048×4, 2.055×2	.006	$O_1, (OH)_1-O_1$	3.112×6, 2.832×4*, 2.816×2* .008
$M_3, M_4-(OH)_3$			$O_1, (OH)_1-(OH)_1$	
Mean	2.050		$(OH)_2, (OH)_3-(OH)_2$	3.112×6, 2.674×4*, 2.622×2* .009
$O_2-(OH)_2$	2.848×4	.020	$(OH)_2, (OH)_3-(OH)_3$	
$O_3-(OH)_3$	2.856×2	.018		
Mean	2.851			
	Angle			*Angle*
O_1-T-O_2	110.45, 110.76		$T-O_2-T$	137.48×2
O_1-T-O_3	110.62		$T-O_3-T$	137.87
O_2-T-O_2	108.38		Mean	137.61
O_2-T-O_3	107.57, 108.98			
Mean	109.46			

* edge shared by two octahedra.

observed diffraction patterns and is unlikely from a structural viewpoint. Just as there are six possible hydrogen bond positions (divided into two sets distinguished by "even" and "odd" numbers in the terminology of Part I) for articulation of a talc sheet on top of a chlorite layer below, there are also six similar positions for placing a brucite sheet on a talc sheet within the layer. Three of these six possibilities correspond to *a* positions and the other three correspond to *b* positions. Random adoption within the different layers of, say, the three *a* sites by a type I brucite sheet would still permit identification of that crystal as being

the Ia structural type. The basis for the original assumption of a fixed brucite position is not valid, but in practice it is impossible to differentiate between the fixed and the random cases. Because of the symmetrical nature of the brucite sheet, in which all atoms repeat at intervals of $b/3$, there will be no difference in the diffraction intensities whether the random $b/3$ interlayer shifts occur relative to both sides of the brucite

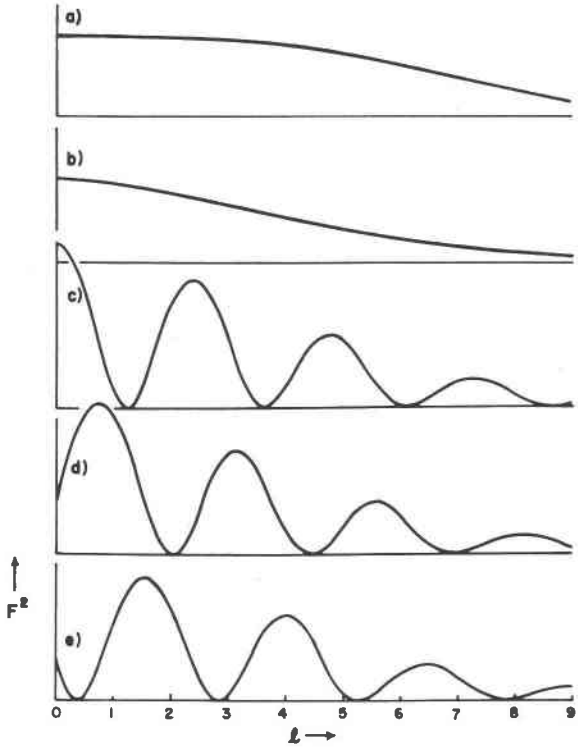

FIG. 1. Intensity distribution along $k \neq 3n$ streaks.

a) "02l," observed.
b) Mean of c), d), and e).
c) 02l, calculated.
d) 1$\bar{1}l$, calculated.
e) $\bar{1}\bar{1}l$, calculated.

sheet or to only one side. There is no diffraction evidence for random displacements of $\pm a/3$ in chlorites. For this reason it is not permissible to mix the a with the b sets in the articulation of one side of the brucite sheet or to mix the "even" with the "odd" sets in articulation of the other side. Despite the inability to recognize interlayer shifts relative to both sides of the brucite sheet, there is no structural validity in well-crystallized chlorites for suggesting that one side of the brucite sheet is

any different than the other side and should be articulated differently to its neighboring talc sheet. Any asymmetric bonding of this sort would imply differences in the two adjacent talc sheets, which is likely to be a rare situation.

Discussion of Refined Structure

The results of refinement indicate that the talc tetrahedral network, which was assumed to be ideally hexagonal at the start of refinement, is distorted by rotations of the tetrahedra in the (001) plane by an average angle of 5.0°, as shown in Fig. 2b. The direction of rotation is such that the basal tetrahedral oxygens move toward the positions of the nearest hydroxyls in the adjacent brucite sheet and away from the octahedral

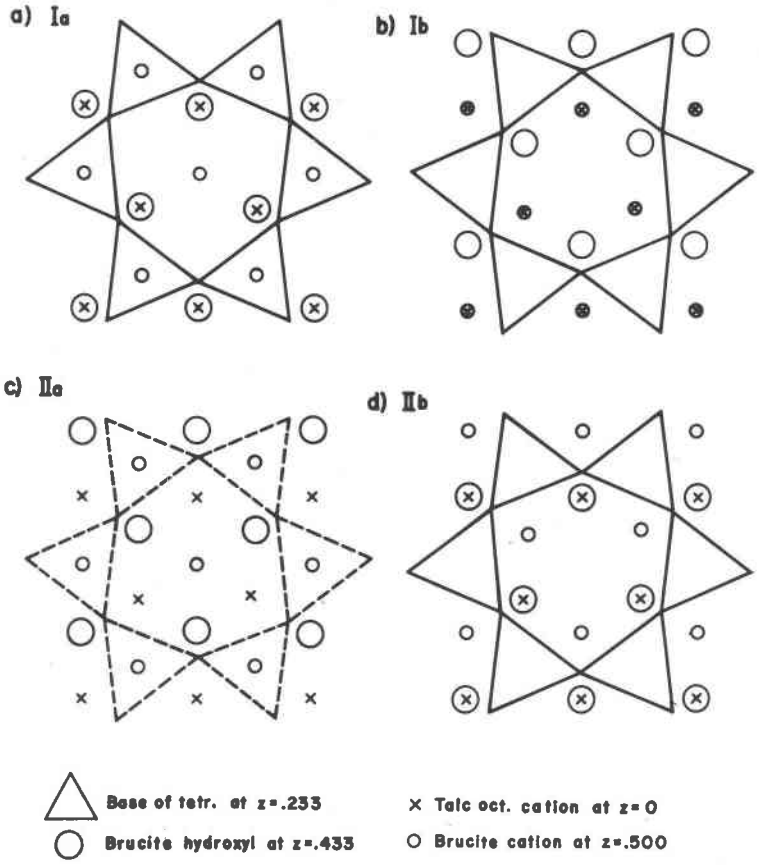

Fig. 2. Structural features of four chlorite layer types in [001] projection, including tetrahedral rotations.

cations in the talc and brucite sheets. In relation to the positions of the talc octahedral cations, this direction of rotation is in the opposite sense to that found in the I*a* and II*b* chlorites (Fig. 2) and also to that in most layer silicates. In Part I it was assumed that the orthohexagonal I*b* structure would have the same direction of rotation of tetrahedra as in the I*a* and II*b* types and, as a result, a relatively unfavorable hydrogen bond distance had been deduced between the talc basal oxygens and the brucite hydroxyls. In the light of the present findings, this conclusion and its implication as to stability of the I*b* structure must be changed. This point is discussed further in the next section.

The angle of tetrahedral rotation (α) can be calculated from a knowledge of the observed b parameter and the ideal tetrahedral b parameter (Radoslovich, 1961) according to

$$\alpha = \cos^{-1}[b(\text{obs})/b(\text{tetr})]. \tag{1}$$

Brown and Bailey (1963) suggest deriving the tetrahedral b parameter for known structures from the measured tetrahedral basal oxygen-oxygen distances A and B.

$$b(\text{tetr}) = (\text{A} + \text{B})\cos(30^\circ + \alpha) + (\text{A} + \text{B})\cos(30^\circ - \alpha), \tag{2}$$

or by untwisting to $\alpha = 0^\circ$

$$b(\text{tetr}) = (\text{A} + \text{B})\sqrt{3}. \tag{3}$$

For the Tazawa chlorite the observed b of 9.336 Å and the ideal tetrahedral b from (3) of 9.374 Å predicts a rotation angle from (1) of 5.2°, which agrees closely with the observed value of 5.0°.

It is known that the (Si, Al)—O distance varies nearly linearly with the tetrahedral Si, Al composition, and standard values of Si—O = 1.62 Å and Al—O = 1.77 Å have been suggested recently for layer silicates by Smith and Bailey (1963). According to these end values, the mean T—O bond length of 1.670 Å for the Tazawa chlorite would be equivalent to $Si_{0.67}Al_{0.33}$ in each tetrahedron. This tetrahedral composition agrees exactly with the value $Si_{2.7}Al_{1.3}$ that was estimated from the basal spacing of 14.166 Å. The symmetry does not allow Si,Al ordering because there is only one independent tetrahedron.

The octahedral composition of the Tazawa chlorite estimated from the b length has 3.4 atoms of Fe per 6.0 actahedral positions. The ρ_o and ρ_o-ρ_c electron density [010] projections indicate that 60% of the Fe is concentrated in the talc sheet. Trial-and-error estimation from the ρ_o-ρ_c maps indicates that Fe makes up 67% of the talc octahedral cations and 47% of the brucite cations. This gives 3.4 Fe per 6.0 octahedral cations, in agreement with the b parameter estimation. The octahedral Mg and Al in the remaining octahedral sites are indistinguishable, but if Mg is

assumed to behave similarly to Fe, then the proportions of the cations in the two octahedral sheets would be:

talc sheet	$Fe_{2.0}Mg_{0.8}Al_{0.2}$
brucite sheet	$Fe_{1.4}Mg_{0.5}Al_{1.1}$

This octahedral composition indicates the excess negative charge due to the substitution of Al for Si in the tetrahedral sheets is compensated primarily by substitution of Al for Fe and Mg within the brucite sheet. Cation ordering within each sheet is not determinable by use of $k=3n$ reflections alone.

The cation compositions of the two octahedral sheets are consistent with the fact that the brucite sheet is thinner than the talc octahedral sheet, 1.98 Å relative to 2.18 Å. Sheet thickness is not a simple function of cation radius alone, because the cation-anion distances and angles in these sheets may also be affected by local charge balance and by structural requirements (Radoslovich, 1963). The difference in sheet thickness is much greater than the difference in average M—O bond length in the two sheets. The brucite sheet appears to be compressed along Z* and stretched in the XY plane because of its greater trivalent ion content and its accordingly greater cation repulsion parallel to (001). The resultant lateral dimensions of the brucite octahedra are identical to those of the talc octahedra (Table 3), so that there is a good fit between the sheets despite the different compositions.

The temperature factors of all the atoms are large, presumably because of the average nature of the structure. In addition, the octahedral cations in both the talc and brucite sheets are elongated approximately parallel to Z* (and Z). The other atoms appear to be isotropic, but this may only be a result of the average structure. It has not been possible to obtain the y parameters of any atoms other than the basal O_2, using only $k=3n$ reflections. Certain of the x parameters are also uncertain because of the 120° layer rotations. As an example, consider the effect of these limitations on the brucite hydroxyls. The O—OH interlayer distance of 2.85 Å obtained using the ideal positions listed in Table 3 is shorter than the 2.90 to 3.00 Å distances found in most other layer silicates. Suppose that each of the three OH groups in an octahedral triad is elongated parallel to Z* and is shifted away from its ideal position in the (001) plane by a small rotation of the triad about Z* so that the actual O—OH distances are about 2.95 Å. The average structure cannot distinguish between the three OH groups and would indicate an average OH centered at its ideal position. This average OH would have a large isotropic temperature factor if the magnitudes of the positional shifts in (001) approximately balance the elongation along Z*. We favor this

interpretation and consider each B value to incorporate the effects both of thermal vibration and of positional shifts. The effect is more marked for the brucite hydroxyls than for the other atoms, as would be expected because of the known rotations of brucite octahedra in other chlorites.

Atom elongation parallel to Z or Z* has not been mentioned for other layer silicates and is not evident on published electron density maps. Thermal vibration should be easier in this direction for a layer structure, but the magnitude of the effect (twice as great along Z as in the XY plane for the octahedral cations) suggests some other factor must also be involved. Octahedral ordering and local charge balance between superposed cations, not determinable by the use of $k=3n$ reflections, may cause some positional variations along Z within each octahedral sheet. These variations would be accentuated in the average structure by the random layer rotations and displacements.

Relative Stabilities

In Part I the relative abundances of the six chlorite structures were interpreted according to their relative stabilities as estimated from two structural features: 1) amounts of repulsion between the brucite cations and the talc tetrahedral cations, and 2) lengths of the hydrogen bonds from the brucite hydroxyls to the talc surface oxygens. The orthohexagonal I*b* structure, the second most abundant variety after the II*b* chlorite,was considered to have a minimum amount of cation repulsion, as does the II*b* type, but to have a relatively unfavorable interlayer hydrogen bond. The O—OH bond length was not known at that time but was deduced from the assumption that the direction of rotation of the talc tetrahedra relative to the talc octahedral cations would be the same as that observed for most other layer silicates. The results of the present study of the Tazawa chlorite, however, indicate that the actual rotation direction is in the opposite sense to the assumed direction and, as a consequence, the orthohexagonal I*b* chorite has a relatively strong hydrogen bond system. The measured O—OH distance of 2.85 Å (Table 3) is slightly shorter than those found for the other chlorite structures, 2.92 Å for the two II*b* polytypes (Steinfink, 1958*a*,*b*) and 2.90 Å for I*a* polytype (Brown and Bailey, 1963), but this value is partly based on ideal coordinates. To a first approximation these distances can be considered to be equivalent and to have little effect on the relative stabilities.

Because the present study suggests that the direction of tetrahedral rotation in chlorites will always be such as to minimize the interlayer hydrogen bond lengths in all chlorite layer types, some additional stability factors must be sought to explain the relative abundances of the

structures. Figure 2 suggests three other structural features that may affect the stabilities:

1) repulsion between the superposed talc and brucite octahedral cations in the I*b* type layer,
2) attraction between the superposed talc octahedral cations and brucite hydroxyls in the I*a* and II*b* type layers, and
3) relative distances of the attractions from the talc surface oxygens to the talc octahedral cations and to the brucite cations.

The first two factors were neglected in Part I of this study because of the six to seven Ångstrom distance over which they must operate. The last factor is dependent on the direction and amount of rotation of the talc tetrahedra. The effects of all the repulsive and attractive forces mentioned are summarized for the four layer types in the chart below, where a plus or minus sign indicates the stability is either enhanced or decreased by the effect.

Atoms concerned	*Distance*	II*b*	I*b*	I*a*	II*a*	*Type of force*
T—M_B	4.4 Å			−−	−−	cation repulsion
M_T—M_B	7.1		−			cation repulsion
M_T—$(OH)_B$	6.1	+		+		cation-anion attraction
M_T—O_S	3.4	+	−	+	(−)	difference of attraction due to rotation of tetrahedra
M_B—O_S	3.9	−	−			difference of attraction due to rotation of tetrahedra

T = tetrahedral cation, M_T = talc octahedral cation, M_B = brucite cation
O_S = talc surface oxygen, $(OH)_B$ = brucite hydroxyl

Repulsion between the superposed brucite and tetrahedral cations is still considered to be the most important structural factor in reducing the stabilities of the I*a* and II*a* layers relative to the I*b* and II*b* layers. This factor alone does not predict any stability differences between I*b* and II*b* layers or between I*a* and II*a* layers. The other interatomic forces listed in the chart suggest that the II*b* layer should be more stable than the I*b* layer and that the I*a* layer should be more stable than the II*a* layer. This gives an order of stability that is in accord with the observed relative abundances of layer types, namely II*b*, I*b*, I*a*, and II*a*.

It is necessary to consider not only the interatomic forces within each type of chlorite layer, but also how the manner of stacking of individual layers to form the six semirandom structures or the several regular polytypes may affect these forces. Figure 3 illustrates in [010] projection the layer sequences and some of the vertically superposed attractive and repulsive forces in these structures. The layer sequences and interatomic force distributions are symmetrical throughout the I*a* ($\beta = 97°$),

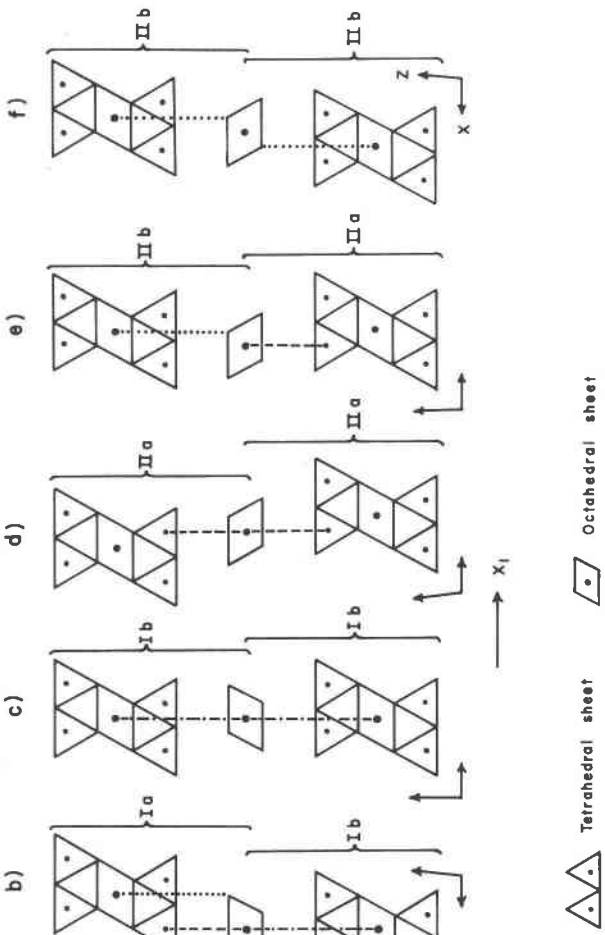

FIG. 3. Schematic diagrams of six chlorite structures in [010] projection. Vertical dashed and dotted lines indicate vertical superposition of atoms.

a) I*a*, $\beta = 97°$.
b) I*b*, $\beta = 97°$.
c) I*b*, $\beta = 90°$.
d) II*a*, $\beta = 97°$.
e) II*a*, $\beta = 90°$.
f) II*b*, $\beta = 97°$.

Ib ($\beta = 90°$), II*b* ($\beta = 97°$), and II*a* ($\beta = 97°$) structures so that the stability ratings in the chart above should be valid for the three-dimensional structures as well as for the individual layers. The I*b* ($\beta = 97°$) and II*a* ($\beta = 90°$) structures are not symmetrical and require special comment. In both of these structures the brucite sheet is positioned asymmetrically so that it bears an *a* relationship to the talc sheet on one side but a *b* relationship to the talc sheet on the other side. In terms of the distribution of interatomic forces the I*b* ($\beta = 97°$) layer sequence is best described as a regular alternation of I*a* and I*b* layers and the II*a* ($\beta = 90°$) sequence as a regular alternation of II*a* and II*b* layers. This emphasizes the fact that there is repulsion between tetrahedral and brucite cations on one side of the brucite sheet but not on the other side for both structures. For this reason the stability of the I*b* ($\beta = 97°$) structure is expected to be lower than that of the orthohexagonal I*b* structure described in this paper, whereas the II*a* ($\beta = 90°$) structure should be more stable than the II*a* ($\beta = 97°$) form. The chart below summarizes the stacking sequences for the six structures and compares their observed abundances with the relative stabilities of the layers involved, 1 through 4 as deduced from the preceding chart.

Polytype	*Stacking Sequence*	*Layer Stabilities*	*Specimens observed in Part I*
I*a*-even, $\beta = 97°$	I*a*+I*a*	3+3	10
I*b*-odd, $\beta = 90°$	I*b*+I*b*	2+2	37
I*b*-even, $\beta = 97°$ (or I*a*-odd)	I*a*+I*b*	3+2	13
II*a*-odd, $\beta = 97°$	II*a*+II*a*	4+4	0
II*a*-even, $\beta = 90°$ (or II*b*-odd)	II*a*+II*b*	4+1	0
II*b*-even, $\beta = 97°$	II*b*+II*b*	1+1	243

The fact that I*b* ($\beta = 97°$) structures do form in nature, despite the alternation of layer types, may be a consequence of the similarity in the relative stabilities of the I*b* and I*a* layers. The reason that the II*a* ($\beta = 90°$) structure is either rare or nonexistent may be due to the large discrepancy in the stabilities of the II*b* and II*a* layers. Alternation of different layer types can also be postulated in the form of *n*-layer packets, which may then be randomly or regularly stacked throughout the crystal. Two-layer packets of this sort have been recognized and will be discussed in a later paper in this series. Shirozu (1958) has recognized alternation of I*b* and II*b* chlorites on a microscopic scale, although in this case the compositions of the two types are not identical. It is interesting to note also that the (001) twinning found to be so common in orthohexagonal I*b* chlorite has the effect of rotating the brucite sheet relative to the talc

sheet and thereby creating a I*b*–II*b* sequence across the twin boundary.

Figure 3a–c helps to explain Shirozu's (1963) observation that orthohexagonal I*b* chlorites readily transform to the monoclinic-cell I*b* or to the I*a* structure on grinding. These transformations only require linear shifts of the talc and brucite sheets relative to one another. Transformation to a II*a* or II*b* structure is structurally more difficult, and would require rotation of the sheets in addition to shifts.

Shirozu also observed that the powder patterns of some unground chlorites containing I*a* and I*b* type layers may be diffuse with broadened and asymmetric 20*l* reflections. This could be due to adoption by a type I brucite sheet of a few wrong stacking positions. For example, a regular sequence of I*b*-odd layers to form the orthohexagonal I*b* structure gives an intense 202 reflection at about 2.50 Å. Introduction of a few I*b*-even sequences in a packet thick enough to give its own diffraction pattern would cause a small peak to form at about 2.44 Å on the shoulder of the 2.50 Å peak. This new peak is the strong $20\bar{3}$ reflection of the monoclinic I*b* chlorite. If the stacking mistakes were distributed instead at random through the crystal, there would be only a single, average $202/20\bar{3}$ peak. It would be broadened and shifted to an intermediate position between 2.50 and 2.44 Å. Similar regular or random systems could also involve introduction of some I*a*-even sequences, for which the strongest 20*l* reflection occurs at about 2.39 Å. It would not be surprising to find stacking mistakes of this sort in I*a* and I*b* type chlorites because of the evidence that these structures result from low temperature, metastable crystallizations.

It was pointed out in Part I that chemical composition may also influence the stability of chlorite structures. The fact that the orthohexagonal I*b* chlorites tend to have high Fe contents (Shirozu, 1960; Bailey and Brown, 1962) may be due to the rotation of the tetrahedra away from the talc and brucite octahedral cations in this structure. It is possible that Fe might be favored in the I*b* relative to the I*a* or II*b* structures because Fe^{2+} is slightly larger than Mg and thereby weaker in its attractive force toward the rotated surface oxygens (Fig. 2). Local balance of electrostatic forces consequent upon tetrahedral and octahedral cation ordering can also influence stability, as suggested by Brown and Bailey (1963) for a I*a* chromium chlorite. The same pattern of ordering and local charge balance has now been demonstrated by a detailed refinement of the I*a* vermiculite structure (Shirozu and Bailey, 1966).

Acknowledgments

The participation in this study of one of us (H. S.) was made possible by a National Science Foundation grant, and of the other (S. W. B.)

by a grant from the Petroleum Research Fund, administered by the American Chemical Society, and by support by the Research Committee of the Graduate School from funds supplied by the Wisconsin Alumni Research Foundation. Computations were carried out in the University of Wisconsin Computing Center, which has also benefited from National Science Foundation support. We are indebted to Dr. Judy Lister for preliminary examination of many of the crystals studied and to Dr. R. A. Eggleton for computing and programming assistance.

References

Bailey, S. W. and B. E. Brown (1962) Chlorite polytypism: I. Regular and semirandom one-layer structures. *Am. Mineral.* **47,** 819–850.

Brown, B. E. and S. W. Bailey (1963) Chlorite polytypism: II. Crystal structure of a one-layer Cr-chlorite. *Am. Mineral.* **48,** 42–61.

Foster, M. D. (1962) Interpretation of the composition and a classification of the chlorites. *U. S. Geol. Survey Prof. Paper* **414-A,** 1–33.

Garrido, J. (1949) Structure cristalline d'une chlorite chromifere. *Bull. Soc. Franc. Mineral. Crist.* **72,** 549–570.

Joel, N., R. Vera and I. Garaycochea (1953) A method for estimation of transmission factors in crystals of uniform cross section. *Acta Cryst.* **6,** 465–468.

Radoslovich, E. W. (1961) Surface symmetry and cell dimensions of layer-lattice silicates. *Nature,* **191,** 67–68.

——— (1963) The cell dimensions and symmetry of layer-lattice silicates. IV. Interatomic forces. *Am. Mineral.* **48,** 76–99.

Shirozu, H. (1958) *X*-ray powder patterns and cell dimensions of some chlorites in Japan, with a note on their interference colors. *Mineral. Jour. (Japan),* **2,** 209–223.

——— (1960) Ionic substitution in iron-magnesium chlorites. *Mem. Faculty Sci. Kyushu Univ., D, Geol.,* **9,** 183–186.

——— (1963) Structural changes of some chlorites by grinding. *Mineral. Jour. (Japan),* **4,** 1–11.

——— and S. W. Bailey (1966) Crystal structure of a two-layer Mg-vermiculite. *Am. Mineral.* (in press).

Smith, J. V. and S. W. Bailey (1963) Second review of Al-O and Si-O tetrahedral distances. *Acta Cryst.* **16,** 801–811.

Steinfink, H. (1958a) The crystal structure of chlorite. I. A monoclinic polymorph. *Acta Cryst.,* **11,** 191–195.

——— (1958b) The crystal structure of chlorite. II. A triclinic polymorph. *Acta Cryst.* **11,** 195–198.

von Engelhardt, W. (1942) Die Structuren von Thuringit, Bavalit und Chamosit und ihre Stellung in der Chloritgruppe. *Zeit. Krist.* **104,** 142–159.

Weisz, O., W. Cochran and W. F. Cole (1948) The accurate determination of cell dimensions from single-crystal *x*-ray photographs. *Acta Cryst.* **1,** 83–88.

Manuscript received, January 4, 1965; accepted for publication, February 16, 1965.